MONITORING RC BRIDGE COLUMN HINGING WITH PHOTOGRAMMETRY

Zeynep Firat Alemdar[1], JoAnn Browning[2] and Jeffrey Olafsen[3], Nick Hunt[4]

[1] *Research Assistant, Department of Civil, Env, and Arch. Engineering, University of Kansas, Kansas, USA*
[2]*Professor, Department of Civil, Env, and Arch. Engineering, University of Kansas, Kansas, USA*
[3]*Professor, Department of Physics, Baylor University, Texas, USA*
[4]*Graduate Engineer, Walter P. Moore and Associates, Inc., Missouri, USA*

Email: zeynep@ku.edu, jpbrown@ku.edu, Jeffrey_Olafsen@baylor.edu, nhunt@walterpmoore.com

ABSTRACT:

A simple photogrammetry method was used to investigate the displacements and rotations of points on column surfaces along the plastic hinging locations in a reinforced concrete bridge structure. Models that are created to represent the hinging behavior in reinforced concrete systems, and the resulting understanding of this behavior under different loading conditions, have traditionally been limited by the ability to validate the model with experimental data. For design and analysis methods leading to reliable performance-based engineering, a better model must be created to predict the extent and locations of nonlinear response in structural systems. As part of this effort, a model of hinging behavior in reinforced concrete bridge systems has been validated using photogrammetric data collected during the NEESR investigation of the seismic performance of four-span large-scale bridge systems at the University of Nevada Reno. The application of photogrammetric techniques in these structural tests used a reference grid on the column surface to record the movement of reference points during strong shaking. The advantages of the applied photogrammetry method are that it is inexpensive and simple to evaluate and can be accomplished remotely. The focus of this paper is the analysis of the photogrammetric data to compare surface deformations and rotations of a reinforced concrete bridge column subjected to dynamic excitation with the results from traditional instruments. The evaluation of the physical behavior of the reinforced concrete bridge column will be described elsewhere.

KEYWORDS: Reinforced concrete bridge column, photogrammetry, hinging regions, rotation.

1. INTRODUCTION

This research evaluates actual hinging behavior in large-scale tests of bridge systems subjected to multiple excitations. A photogrammetric method was used to remotely track deformations of the concrete surface in the hinging regions. Photogrammetry is a non-invasive technique of remote visualization of the target components and a computer rendering of the motion (Jauregui et al. 2006). This computer reconstruction is based on the tracked motion of the target components which are discrete points on the column surface. Photogrammetry measurements were taken in two hinging regions: at the bottom and top level of the column. The main objectives were to provide the lateral displacements of points on the column surface over a continuum and to calculate the vertical and cross-sectional rotation between these points. This paper focuses on the analysis of simple and inexpensive photogrammetric data from a large-scale dynamic test of a reinforced concrete bridge system. The evaluation of the physical behavior of the reinforced concrete bridge column will be described elsewhere.

2. FOUR-SPAN LARGE SCALE RC BRIDGE TEST

The four-span large scale reinforced concrete bridge was tested on February 12-15, 2007 at the University of Nevada Reno (UNR) laboratory. The significance of this test was that it was a large-scale bridge system with columns

having double curvature response and resisting massive earthquake motions.

The test specimen consisted of a four-span reinforced concrete bridge with end abutments as shown in (Fig. 2.1). The bridge was quarter-scale with two interior spans that were 29 ft (8.84 m) in length, and two exterior spans of 24.5 ft (7.47 m) for a total length of approximately 110 ft (33.5 m). The clear heights of the bents were 5, 6 and 7 ft (1.52, 1.83, and 2.13 m), with the tallest bent in the middle (Bent 2). The superstructure consisted of a solid slab that was post-tensioned in both the longitudinal and transverse directions. The bridge also included abutment seats at both ends that were driven in the longitudinal direction by dynamic hydraulic actuators. The depth of the cap beams was 15 in. (0.38 m). The total length of the cap beams (perpendicular to the longitudinal axis of the bridge) was 98 in. (2.49 m). The concrete compressive strength used in the bridge (excluding the slab) was 6.7 ksi and reinforcement was ASTM A706 Grade 60. The bents were numbered Bent 1, Bent 2, and Bent 3 starting from left (South) to right (North).

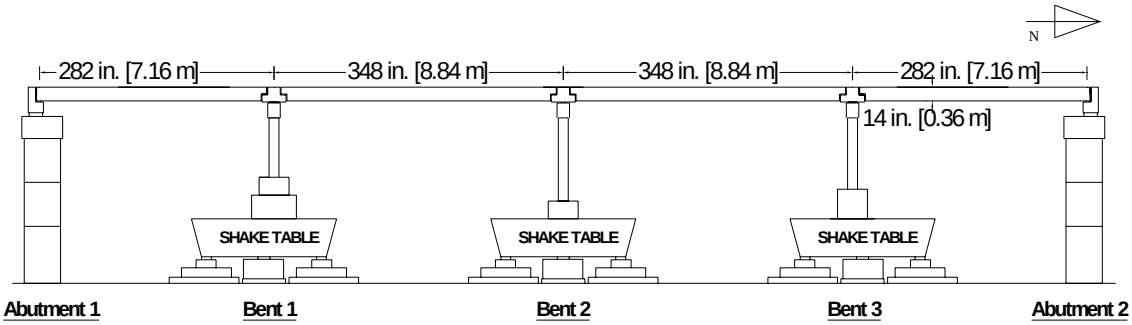

Fig. 2.1 Elevation view of the four-span bridge

The top and bottom hinging regions of the east column of Bent 3 were the focus for collecting photogrammetry data in the large-scale four-span reinforced concrete bridge test. Two grid systems were applied (Fig. 2.2). The bottom grid consisted of vertical and horizontal lines spaced irregularly around the face of the circular column. The top grid used a different configuration consisting of lines and squares that resembled the spacing of the lines in the bottom grid. The top grid was applied to simulate “targets” on the column surface, whereas the bottom grid represented continues lines with intersecting points. It was determined through the reduction of the photogrammetry data that Points were best defined as the intersections of the thick vertical and horizontal lines in both regions, as shown in Fig. 2.3. The locations of a series of linear vertical displacement transducers (LVDTs) and one displacement transducer (DT7) monitored by the research team at UNR are also shown in the figure.

(a) (b)

Fig. 2.2 Close view of (a) bottom and (b) top grid systems

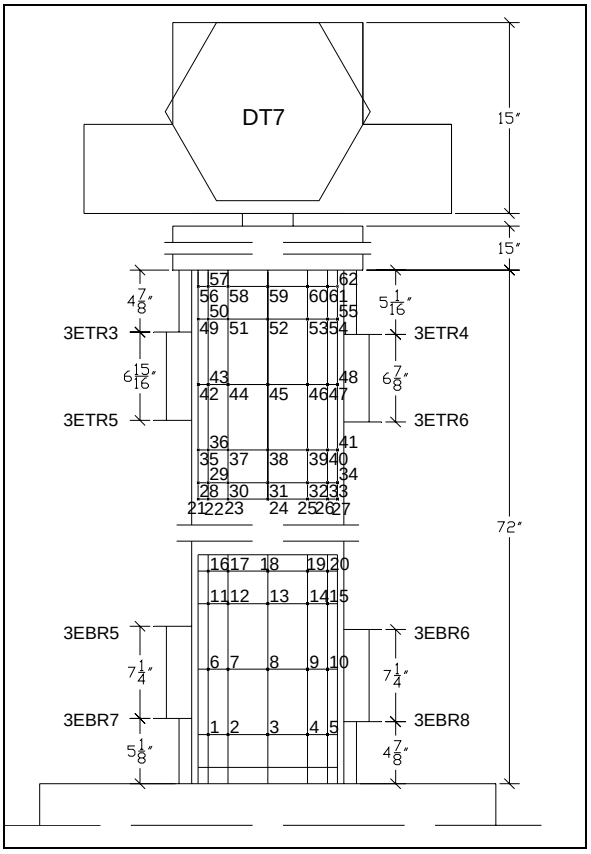

Fig. 2.3 Grid system and LVDT locations on column in the Bent 3 east column

An aluminum tower was used to place cameras to record the earthquake events. The tower had two levels to photograph the plastic hinging regions. A system of two cameras (DXB-9212EF model Starlight 600 TVL super high resolution) with black-white recording properties was mounted on each level. Video-lens zooms having 60-300mm F4-5.6 capturing capability were also used. The earthquake motion used in the tests consisted of biaxial and uniaxial applications of scaled motions measured at the Century City Country Club during the 1994 Northridge, California earthquake. This motion was applied 13 times with six different scaled intensities of increasing amplitude so that the progression of damage could be tracked from pre-yield to failure.

3. DEFINITION OF POINTS ON COLUMN SURFACE

Displacements and cross-sectional rotations of locations on the column were tracked during the earthquake events. For each measurement, it is necessary to have a consistent and predictable definition of points on the column surface. There are some challenges in the photogrammetry analysis due to some degraded images and the reliability of the selected method to define the points on the column surface. In addition, there are some differences in the data provided by LVDT instrumentation and that recorded for the photogrammetry application. One difference is that the rotation calculations obtained using photogrammetry analysis represents the cross-sectional rotations based on the movement of the column, which includes not only flexural but also rigid body rotation. Rotations calculated using the LVDT data from the test includes only flexural contributions. Another difference is that the LVDT instrumentation was set to record movement in the transverse and longitudinal planes, and photogrammetry measurements were recorded at an angle between the LVDT instrumentation. This difference in orientation is accounted for in the analysis and results.

3.1. Unclear Images

The image (640 x 480) was written as 480 lines that are 640 pixels wide. Each image represents 1/30th of a second during the test. The images are interlaced: The odd-numbered lines are written first, followed by the even-numbered lines so that the image is really two images offset by 1/60th of a second. The first "partial image" (half of the total image) is comprised of the odd lines, and the second "partial image" is comprised of the even lines. Due to the shaking effect from the strong floor during the tests and the incompatibility in recording frequency between the cameras and the earthquake motions, many images were compromised. Some of the images appeared as double lines for each horizontal and vertical line, and some were simply blurry images.

One option to improve calculations of displacements and rotations using the corrupted images is to consider only the even-numbered or odd-numbered lines, separately. If the even and odd lines are separated, the double image effect that is produced by a shift between the two halves of the image being written can be avoided by considering only one "half image" at a time. The vertical displacement results of Point 7 (as shown in Fig. 2.3) in the even and odd line analyses during Test 4D motion, which has a peak ground acceleration of 0.5g in transverse direction and 0.6g in longitudinal direction, are compared with the LVDT 3EBR7 reading in Fig. 3.1-3.2. Because of the larger disparity noted in the figures between peak displacement values recorded in the odd-line analysis (Fig. 3.2) and LVDT recordings, the even line approach (Fig. 3.1) is selected to provide better photogrammetry results.

The cross section rotations calculated using photogrammetry measurements and those determined using the LVDT data are shown in Fig. 3.3. Cross section rotation is calculated as the relative vertical displacements between points 7 and 8 divided by the horizontal distance between the points. For the photogrammetry analysis, the horizontal distance between the points changes within each image. The rotation data obtained using LVDTs are for a specific location on the column face, and the horizontal distance between the LVDTs is assumed to be constant. Figure 3.3 shows the comparison of the cross-sectional rotations between the photogrammetry values and the rotation derived from LVDT data at 12 inches from the bottom fixity in the transverse direction. The general periodicity and peak values of response are similar between the LVDT and photogrammetry results. The appearance of "noise" with nearly constant magnitude is a result of single pixel differences in calculated displacements (pixelization).

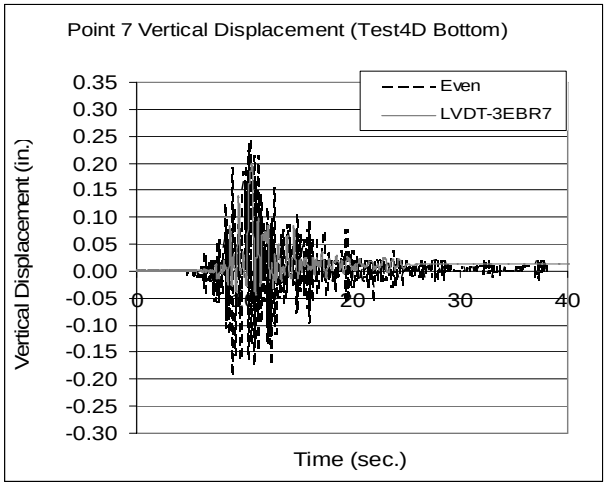

Fig. 3.1 Comparison of Point 7 vertical displacement for even lines with LVDT 3EBR7 data

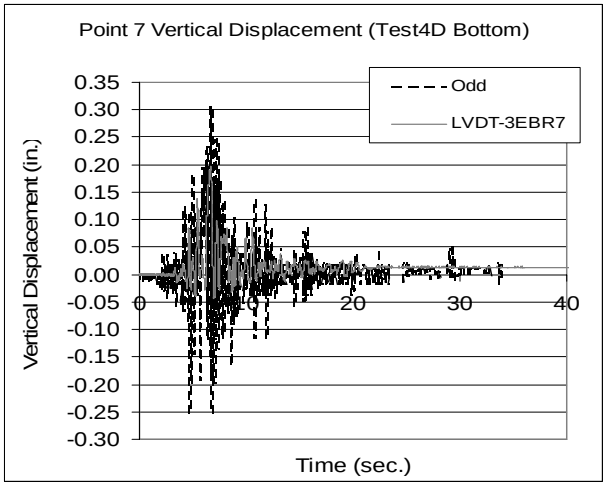

Fig. 3.2 Comparison of Point 7 vertical displacement for odd lines with LVDT 3EBR7 data

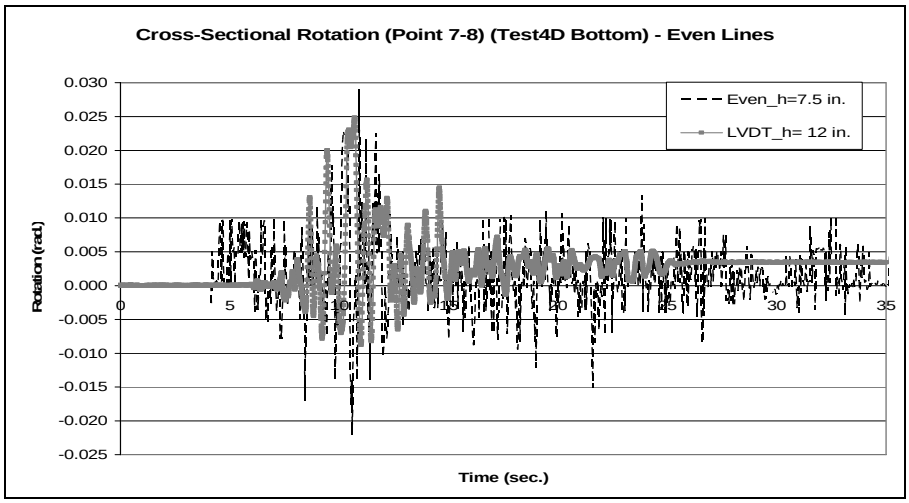

Fig. 3.3 Cross-sectional rotation between Points 7 and 8 at the bottom grid compared with LVDT rotation at 12 in. from the bottom fixity in the transverse direction

3.2. Intersecting Lines

There are several options for defining each unique point on the grid. Points on the grid are defined by the intersection of the thick vertical and horizontal lines (0.25 in. thick). Therefore, there are several ways to define a line within that thickness. One option is to seek a definition of the mid-point of each 0.25-in. thickness and define a "middle line" as the connection of those points (Fig. 3.4). Another option is to define the edges of the lines. For this option, the "edge lines" may be defined by points of a particular light intensity value (Robert Threshold) or a change in relative intensity between the black to white paint transition. Finally, the length of the line that is used to define each Point on the grid also will influence results. The best representation of a Point was found to be the average of four points. First, the edge-lines of the 0.25-in. thick grid lines were used to define four corner points at the intersection of each horizontal and vertical grid line. The horizontal and vertical grid lines were defined using a constant Robert threshold value with a length ranging from 0.5-1.5 in. The corner points were then averaged to define a "middle point".

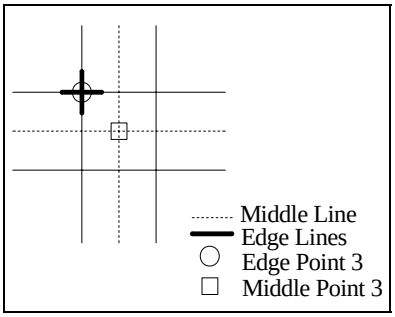

Fig. 3.4 Close up of lines used to define Point 3 (Fig. 2.3)

3.3. Vertical Rotation vs. Cross-Sectional Rotation Calculation

The vertical rotation for the column can be calculated using transverse movements of two points that are aligned vertically, which represents the average cross-sectional rotation between those two points if shear deformations can be neglected. To see the difference between calculated vertical rotations and cross-sectional rotations, transverse movements of points on the bottom grid system were determined. The vertical rotation was calculated using the relative lateral displacements of two vertically-aligned points on the grid surface divided by the vertical distance between the points.

The lateral displacements of Point 3 and 8 on the bottom grid were tracked during Test 4D motion to calculate vertical rotations (Fig. 3.5). Points 7 and 9 shown in Fig. 2.3 were selected and the vertical movements of the Points were determined to calculate the cross-sectional rotation during Test 4D. The comparison between the cross-sectional rotation results and the LVDT cross-sectional rotation values that are obtained using LVDT 3EBR7 and 3EBR8 data is shown in Fig. 3.6. The vertical rotation results (Fig. 3.5) follow the LVDT cross-sectional rotations well and provide a much smoother representation than the cross-sectional rotations. Although the vertical rotations are average rotations over a given height, the results show much better peak values and periodicity when compared with LVDT calculations (Fig. 3.5-3.6).

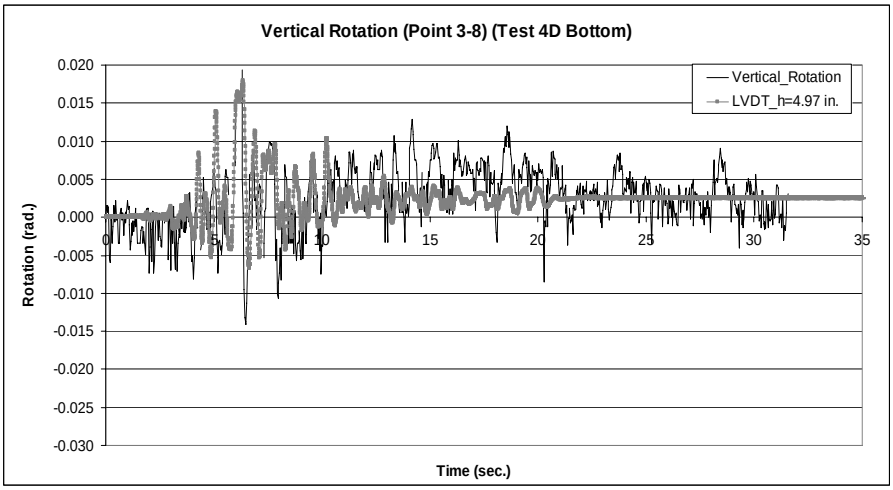

Fig. 3.5 Vertical rotation calculated using Point 3 and 8

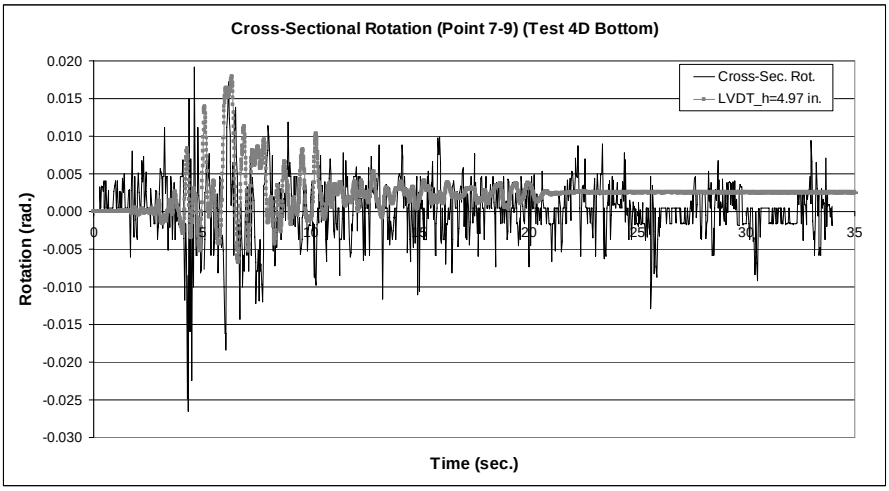

Fig. 3.6 Cross-sectional rotation using Point 7 and 9

3.4. Displacement Calculations of the Grid Points

The transverse (Fig. 3.7) and vertical displacements (Fig. 3.1) are calculated at each of the grid points along the hinging surface. The deformed shape of the hinging regions can now be defined over a continuum by considering the movements of the defined Points. The deformations in the hinging regions during Test 4D are compared in Figs. 3.8 and 3.9 with the associated column images at the time of maximum column drift.

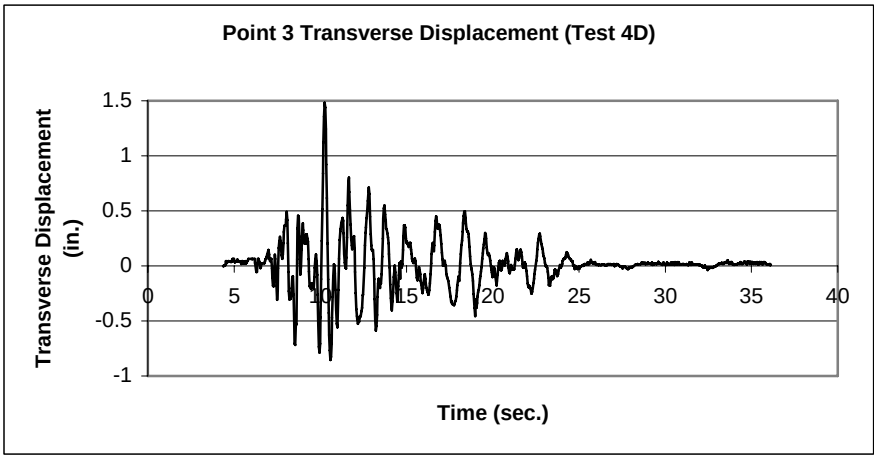

Fig. 3.7 Transverse displacements of Point 3 during Test 4D motion

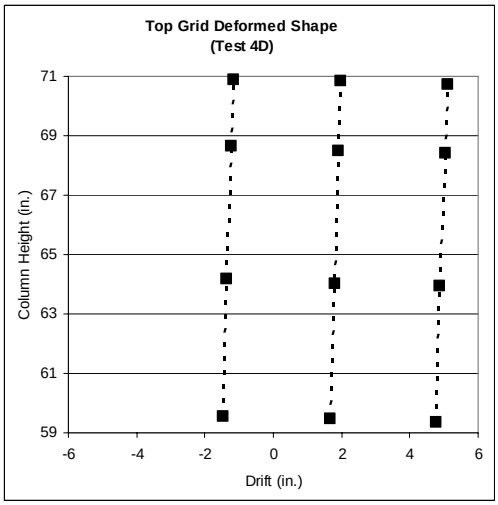

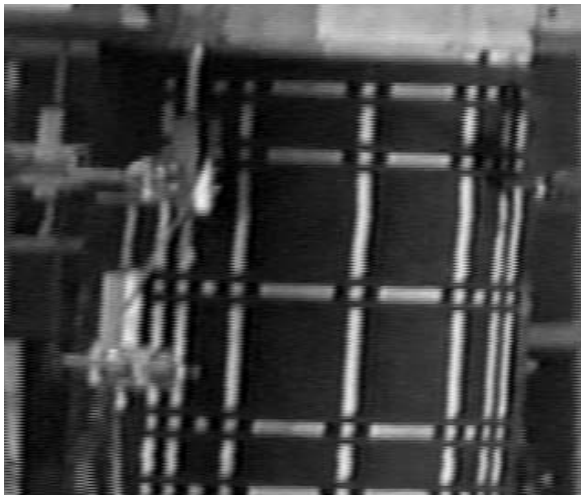

Fig. 3.8 Top grid deformed shape with picture comparison at maximum column drift

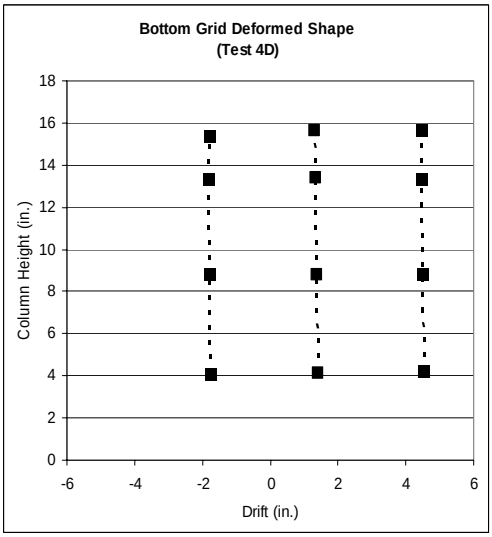

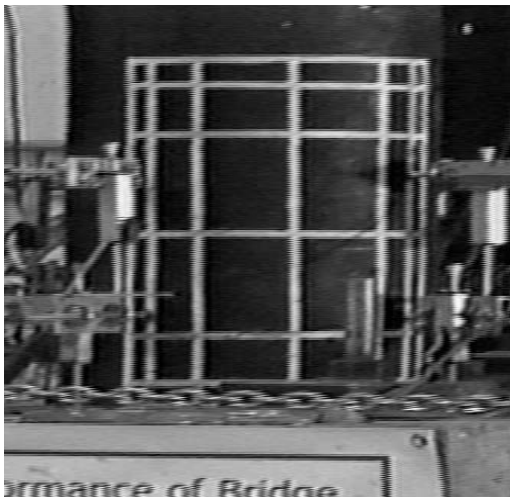

Fig. 3.9 Bottom grid deformed shape with picture comparison at maximum column drift

4. CONCLUSION

Deformations of the bridge column surface during response to strong ground motion were successfully reconstructed using simple photogrammetry data. For each deformation calculation, it is necessary to have a consistent and predictable definition of points on the column surface. The quality of images captured during the test and the similar pixel intensities across the grid line thickness presented challenges for calculating consistent displacement and rotation results. The following conclusions are made regarding the analysis of the deformations in the hinging region during response to strong ground shaking:

- The best image quality is obtained by using the even-numbered lines from each frame in time. In the future tests, cameras that operate using progressive scan rather than interlaced images when recording the events should be used.
- The edges of the 0.25-in. thick grid lines are best defined using a constant Robert threshold value.
- The best definition of a unique point on the column surface is obtained by using the edge-lines of the 0.25-in. thick grid lines to define four corner points at the intersection of each horizontal and vertical grid line, and then averaging these points to define a “middle point”. The edge-lines are best defined using lengths of 0.5-1.5 in.
- The vertical rotations calculated using photogrammetry data, as an average rotation between two consecutive grid points, represent the cross-sectional rotations calculated using the LVDT data in periodicity very well. The traces are smoother than the detailed cross-sectional rotation calculation from photogrammetry data. The maximum amplitude of rotation is similar between vertical and cross-sectional rotation calculated using the photogrammetry data.

REFERENCES

Jauregui D., Ruinian J., K. White. 2006. “Review of Close-Range Photogrammetry Applications in Bridge Engineering”, Washington, D. C. Transportation Research Board, Washington.

Acknowledgements

This project gratefully acknowledges the support of NSF grant #0532084, Joy Pauschke Program Director. The assistance and support of Prof. Saiid Saiidi, Graduate Research Assistant Roby Nelson, the entire staff of the research facilities at the University of Nevada Reno, and Graduate Student Nick Hunt at University of Kansas are also gratefully acknowledged. Prof. Olafsen was supported in part by a Big XII Faculty Fellowship. Additional support from KU Transportation Research Institute is gratefully acknowledged.